Microplastics exacerbate virus-mediated mortality in fish

Meredith Evans Seeley[1]†*, Robert C. Hale[1], Patty Zwollo[2], Wolfgang Vogelbein[1], Gaelan Verry[1], Andrew R. Wargo[1]

Affiliations:

[1]Virginia Institute of Marine Science, William & Mary, Gloucester Point, VA 23062

[2]William & Mary, Department of Biology, Williamsburg, VA 23187

*Correspondence to: meseeley@vims.edu

†Present affiliation: National Institute of Standards and Technology (NIST) and Hawaii Pacific University Center for Marine Debris Research, Waimanalo, HI 96825
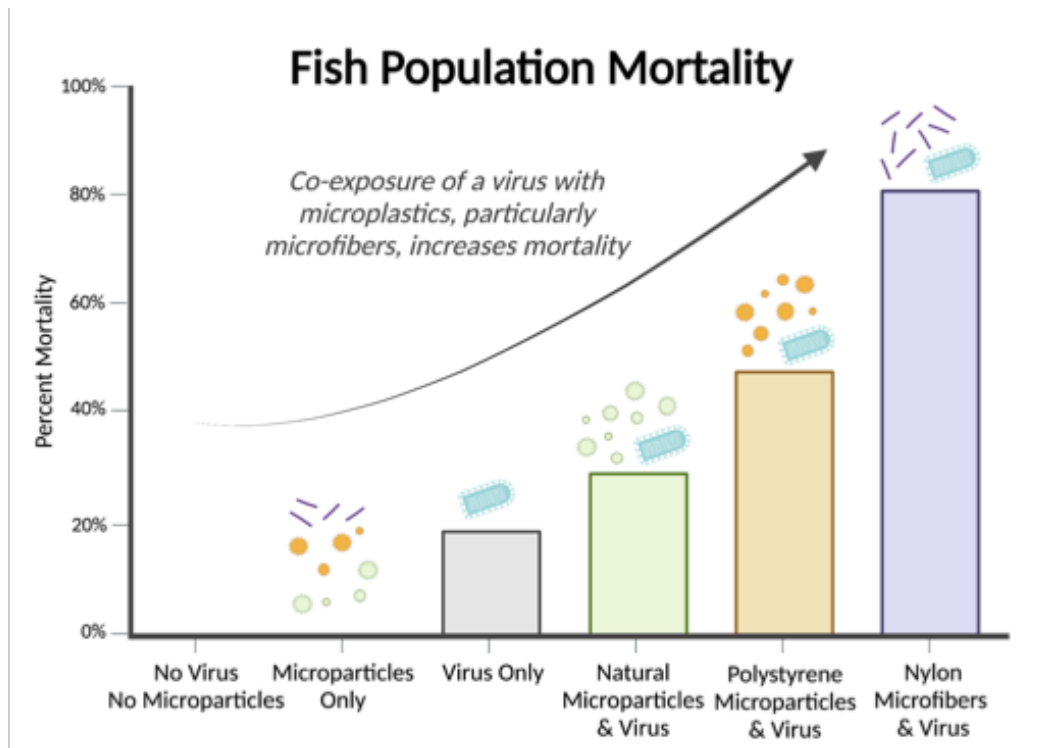
14   **Abstract:** Microplastics are a persistent and increasing environmental hazard. They have been

15   reported to interact with a variety of biotic and abiotic environmental stressors, but the

16   ramifications of such interactions are largely unknown. We investigated virus-induced

17   mortalities in a commercially important salmonid following exposure to microplastics, plastic

18   microfibers, and natural (non-plastic) microparticles. Microplastics or microparticles alone were

19   not lethal. Mortality increased significantly when fish were co-exposed to virus and

20   microplastics, particularly microfibers, compared to virus alone. This presents the unique finding

21   that microplastics (not natural microparticulate matter) may have a significant impact on

22   population health when presented with another stressor. Further, we found that mortality

23   correlated with host viral load, mild gill inflammation, immune responses, and transmission

24   potential. We hypothesize that microplastics can compromise host tissues, allowing pathogens to

25   bypass defenses. Further research regarding this mechanism and the interplay between

26   microplastics and infectious disease are paramount, considering microplastics increasing

27   environmental burden.

28   **Keywords:** microplastics, microfiber, virus, co-stressor, aquaculture, rainbow trout

29

30   **Graphical Abstract**

Fish Population Mortality

Co-exposure of a virus with microplastics, particularly microfibers, increases mortality

Percent Mortality (y-axis): 100%, 80%, 60%, 40%, 20%, 0%

Categories (x-axis): No Virus No Microparticles, Microparticles Only, Virus Only, Natural Microparticles & Virus, Polystyrene Microparticles & Virus, Nylon Microfibers & Virus

31

1. Introduction

32

33   Plastic production, use, and environmental release are increasing worldwide. Despite

34   their longevity, plastics may weather and fragment into microplastics ($\leq$ 5mm) over time. This

35   has led to the ubiquitous accumulation of microplastics in aquatic, terrestrial, and atmospheric

36   environments (Borrelle et al., 2020; Geyer et al., 2017; Hale et al., 2020). Humans are also

37   exposed and microplastics have recently been detected in human blood and placenta (Leslie et

38   al., 2022; Ragusa et al., 2021). While long presumed to be toxicologically inert, research

39   suggests that plastic pollution presents health risks to living resources and humans (Bucci et al.,

40   2020). Oversimplification of microplastics as a single homogeneous contaminant, however,

41   ignores their toxicological complexity, as microplastics vary in size, shape, density, polymer

42   chemistry, additive composition, and more (Rochman et al., 2019). Available research suggests

43   that many effects of microplastics are sub-lethal and derive from their physical and chemical

44   characteristics (Bucci et al., 2020; Zimmermann et al., 2019). Further, to date, the relative

45   toxicities of naturally occurring polymeric microparticles (e.g., cellulose-based) have been rarely

46   investigated despite their abundance in the environment. Thus, our ability to evaluate the

47   toxicological significance of exposure to synthetic microplastics versus other microparticles is

48   limited. Similarly, microfibers (as opposed to spheroidal microplastics) have been less

49   commonly investigated despite their dominance in some environments (Athey and Erdle, 2021).

50   It has been postulated that microplastics may act in concert with other stressors, such as

51   causative agents of infectious disease (pathogens) (Lamb et al., 2018; Leads et al., 2019;

52   MacLeod et al., 2021). Indeed, pathogen fitness and virulence (i.e., infection-related morbidity

53   and mortality) can be influenced by environmental pollutants (Springman et al., 2005). For

54   example, prevalence of plastic debris and disease were reported to be correlated in Asian Pacific

55   corals (Lamb et al., 2018). Possible mechanisms include, but are not limited to: plastics act as a

56   sterile vector for pathogens (Amaral-Zettler et al., 2020); interactions of hosts with plastic causes

57   tissue damage and has deregulatory or pro-inflammatory effects on the immune system (Hale et

58   al., 2020; Zwollo et al., 2021); or coincident plastic, chemical (including contaminants sorbed to

59   the plastic surface), pathogen (e.g., arising from local human populations), and/or other

60   pollutant(s) combine to compromise the host. Available research is limited and has not yet

61   adequately clarified these interactions (Lamb et al., 2018; Leads et al., 2019). Considering the

62   ubiquity of microplastic pollution and pathogens in the environment, more research is warranted

63   to protect valuable resources. This is especially true for fisheries and aquaculture species, whose

64   environments can be both pathogen- and microplastic-laden (Jennings et al., 2016).

65   Here, we probed the effects of microplastics alone or with co-exposure to an aquatic virus

66   of worldwide concern, infectious hematopoietic necrosis virus (IHNV), on a species of

67   commercial and conservation relevance, rainbow trout (*Oncorhynchus mykiss*). This is a well-

68   studied virus and host, as IHNV leads to significant financial and ecosystem losses globally for

69   multiple types of salmonid species (Bootland and Leong, 2011; Dixon et al., 2016). We

70   evaluated resulting fish mortality and possible underlying histopathological and immunological

71   mechanisms. Microparticles included a polystyrene microplastic (expanded polystyrene, ground

72   and sieved to ~20 µm), nylon microfiber (10 x 500 µm flocking fibers), and a natural

73   microparticle, 'spartina' (marsh grass, *Spartina alterniflora*, washed, high-temperature dried,

74   ground, and sieved to ~20 µm). Microplastics were selected with consideration for the variety of

75   plastics that are used intensely in fisheries activities (e.g., polystyrene buoys and floats, nylon

76   nets or lines), as well as other sources. For example, polystyrene originating from building

77   insulation and single-use food containers is also commonly observed in stranded debris and

78 nylon fibers are widely used in textiles. Fish were exposed to microparticles in water at one of

79 three concentrations over eight weeks. After four weeks, half of the fish were acutely exposed by

80 immersion to a controlled dose of IHNV. For each treatment, fish were monitored for *in vivo*

81 mortality and viral shedding. A fourth tank for each high particle concentration and controls

82 (IHNV+ and -) was maintained for destructive sampling to analyze tissue viral load,

83 histopathology, and immunological markers over time. We hypothesized that chronic exposure

84 to polystyrene microplastics and nylon microfibers would increase IHNV virulence (compared to

85 fish co-exposed to virus alone, or to the natural microparticle and virus), and that insights into

86 the mechanism underlying virulence changes, as well as population level impacts, could be

87 gained from viral load/shedding, histopathological and immunological analyses.

88 **2. Methods**

89 *2.1 Particle Preparation*

90 Expanded polystyrene foam, commonly used as building insulation, was purchased from

91 a local houseware store. Foam was embrittled and ground in a Retsch CryoMill, sieved to ≤20

92 µm with Retsch AS 200 air jet sieve and Gilson Performer III Sieve shaker (Seeley et al., 2020).

93 *Spartina alterniflora* (marsh cordgrass) was collected from estuarine marshes near Yorktown,

94 VA by cutting dead stems near the base. Grass was sorted in a fume hood, washed with

95 deionized water, and dried in a muffle oven at 60˚C. Sections were ground in a blender, then the

96 Retsch CryoMill, and sieved as above. Undyed nylon 6'6 fibers were obtained from Claremont

97 Flock, Inc. Fibers measured 0.8 denier (approximately 10 µm) in diameter and 0.5 mm in length.

98 Size ranges of the particles were measured using a Beckman-Coulter Laser Diffraction Particle

99 Size Analyzer, which measures the longest diameter of a particle. Photo-flo (© Eastman Kodak

100 Company) was added to the particle/water mix to increase dispersion and decrease particle

101 clumping for analysis with the particle size analyzer (not in experiment). Particle size analysis

102 confirmed the 500 x 10 μm measurement of nylon fibers provided by the manufacturer. The

103 median diameter of polystyrene particles was 26.8 μm; 25% of particles were less than 16.4 μm.

104 The median diameter of spartina particles was 39.2 μm; 25% of particles fell below 21.3 μm.

105 Particle size analysis and microscopic images of particles are provided in Fig. S1. The data

106 illustrated that spartina contained longer particles than polystyrene (a product of the plant

107 cellular structure) which passed through the sieve via their shortest axis; this and any potential

108 clumping may account for the overall greater size particles than polystyrene despite using the

109 same sieving approach. The laser analyzed the nylon fibers at different orientations in the fluid.

110 This likely accounts for the wide range of diameters measured. However, the predominance of

111 measurements of 10 and 500 μm supported our expectation that these were the primary size axes

112 of the nylon fibers (as provided by the manufacturer). The particles displayed similar behaviors

113 and buoyancy in the experimental tanks, characterized by a brief period of floating on the water's

114 surface (less than 10 minutes) and ultimately distributing within tank, a result of mixing from

115 aeration.

116 *2.2 Experimental Design and Procedures*

117 Fertilized eyed rainbow trout (*Oncorhynchus mykiss*) eggs were obtained from the

118 National Center for Cool and Cold Water Aquaculture in West Virginia (NCCCWA; within

119 USDA's Agricultural Research Service). Trout were hatched and reared at the Virginia Institute

120 of Marine Science (VIMS), according to guidelines from the Institutional Animal Care and Use

121 Committee (IACUC-2020-06-24-14322-arwargo) and previously established protocols (Everson

122 et al., 2021). Briefly, fish were maintained at 1-3% weight food, fed daily. Fish were initially

123   held in a specific pathogen-free recirculating system supplied with UV-irradiated fresh well-

124   water at 12 ± 1°C until reaching the desired size for experiments.

125   For the experiment, fish were transferred to a flow-through tower rack tank system

126   (Aquaneering) housed in a BSL-II aquatic animal laboratory at VIMS, supplied by UV-irradiated

127   fresh well-water at 15°C. Room air temperature was maintained at 15.8 ± 0.4°C, water

128   temperature at 15.0 ± 0.2°C, dissolved oxygen at $100.1 \pm 0.5\%$ saturation, and lighting on a 12-

129   hour diurnal cycle. Fish were housed in 6 L tanks (20 fish each) with one water line, two air

130   stones, and fry screens, to facilitate particle circulation and oxygenation through the entire tank.

131   Water flow rate was set to 300-350 mL min^{-1}. During the experiment, fish were fed 2.0% of

132   their average body weight every four days, 1 hour after the start of a tank flush with fresh water

133   (below). Average fish weight was 5.2 ± 0.4 g fish^{-1} at the start of the experiment.

134   Fish received one of 20 possible treatments, outlined in Fig. 1 and Table S1. Each

135   treatment contained triplicate tanks of 20 fish tracked for mortality and sampled for viral

136   shedding. A fourth replicate was included for destructive tissue sampling in the high particle

137   treatments and controls. Treatments and replicate tanks were randomly distributed throughout the

138   tower rack system. For plastic exposure, fish were dosed with particles every other day,

139   beginning on the first day of the experiment. In the first half of the experiment (weeks 1-4, prior

140   to IHNV exposure) water in all tanks was held static for 24 hours during particle exposure. The

141   flow was then resumed and tanks flushed for 24 hours to maintain water quality. Fish were

142   switched to clean tanks after two weeks to remove buildup of feces debris and reduce ammonia

143   levels (water ammonium maintained $\leq$5-8 ppm). In the second half of the experiment, the static

144   plastic exposure period was reduced from 24 to ~10 hours, followed by a 38-hour flushing period

145   rather than conducting tank changes to reduce risk of contamination of IHNV across tanks. In

146   total, the experiment lasted 56 days with 28 particle dosing events. Day 1 was considered the

147   first day of fish exposure to microplastics. The experiment was monitored at the same time daily,

148   recording temperature and dissolved oxygen continuously on YSI probes, and manually

149   inspecting the number of fish mortalities in each tank.

Microparticle Concentrations: Low (0.1 mg L⁻¹), Med (1 mg L⁻¹) or High (10 mg L⁻¹)

x 3
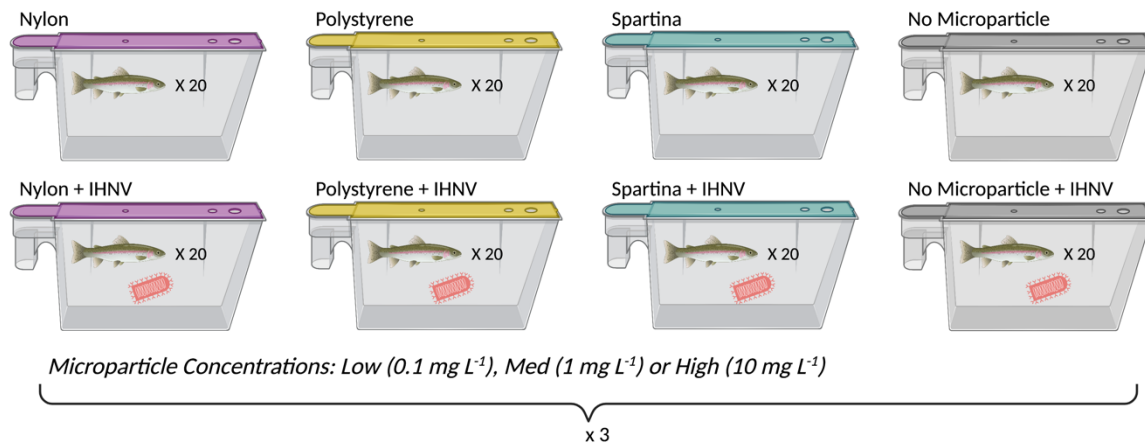
150   **Fig. 1** Experimental design, consisting of 20 possible treatments. Fish were exposed to no

151   microparticles or microparticles at one of three concentrations, in the presence or absence of

152   virus. The high dose microparticle treatments and no particle treatments (IHNV+ and -) had a

153   fourth replicate for destructive sampling, resulting in 68 tanks total (Table S1).

154

155   To reduce microplastic discharge to the local wastewater system, during the first hour of

156   each tank flushing effluent was pumped through a series of in-line filters (75 µm, 20 µm, 5 µm

157   and 1 µm), before passage through UV-irradiation (sufficient for virus inactivation) and eventual

158   discharge to the municipal wastewater system.

159   Halfway through the experiment (day 28), fish were dosed with virus or a mock control.

160   Experimental virus, IHNV (*Salmonid novirhabdovirus*) isolate C (genotype mG119M; GenBank

161   accession number AF237984) was obtained from established laboratory stock (titer of 7.56×10^8

162   plaque forming units (PFU) mL^{-1}) diluted to 1.0×10^6 PFU mL^{-1} in Minimum Essential Media

163   (MEM) with 10% fetal bovine serum (Jones et al., 2020). Fish were dosed with 5 mL of diluted

164   IHNV stock in 995 mL water, to reach a final IHNV dose of 5.0×10^3 PFU mL^{-1}, in a 1-hr static

165   immersion challenge, followed by resumption of water flow to the tanks(Jones et al., 2020).

166   Non-virus (IHNV-) treatments were mock dosed with 5 mL of MEM with 10% fetal bovine

167   serum.

168   To quantify viral shedding, 800 µL water samples were collected on days 28, 30, 32, 34,

169   36, 38, 40, 42, 48, and 54, from each of the triplicate survival analysis tanks per treatment. Water

170   was collected at the end of the static period just prior to flushing, such that virus had maximum

171   and consistent time to accumulate in tanks, then stored at -80˚C prior to extraction and analysis.

172   A 210 µl volume of sampled water then underwent RNA extraction and quantitative real time

173   polymerase chain reaction (qPCR) for IHNV quantification as detailed in Jones et al. 2020.

174   Tissue samples were collected following virus exposure on day 31, 35, 42 and 56 (3, 7,

175   14, and 28 days post-virus respectively; Fig. S2). Five fish were euthanized via overdose of

176   tricaine methanesulfonate (MS-222) from each tissue sampling tank (Table S1) on each

177   dissection day. On day 56 some tissue sampling tanks had less than 5 survivors, so fish were

178   collected from survival analysis tanks of the same treatment, since it was the last day of the

179   experiment and survival no longer needed to be tracked (number collected from another tank in

180   no particle IHNV-: 3; no particle IHNV+: 3; spartina IHNV+: 2; polystyrene IHNV+: 4; nylon

181   IHNV+: 5). Fish were weighed, and dissected following standard procedures to excise two gill

182   arches (left side) and the anterior kidney (Gauthier et al., 2021). One gill arch and approximately

183   100 mg of anterior kidney tissues were preserved separately in 750 uL of RNAlater

184   (ThermoFisher) for viral load and immune marker analysis and stored until RNA purification at -

185   80˚C. A second gill arch was preserved in a buffered formalin fixative (Z-Fix, Anatech) for

186   paraffin histology.

187   Routine methods of paraffin histology were used for the analysis of gill arches (Gauthier

188   et al., 2021). Briefly, individual gill arches were washed, decalcified, dehydrated in a graded

189   series of ethanols, cleared in xylene substitute, and embedded in paraffin wax. Tissue blocks

190   were sectioned to 5 μm with a rotary microtome, stained with haematoxylin and eosin, and

191   prepared slides were evaluated on an Olympus AX-70 photomicroscope, focusing analysis on the

192   best-preserved section of gill tissue for each sample. A severity scale 0-3 was applied for semi-

193   quantitative comparison between samples, where 0: no pathology observed, 1: mild (low-density

194   mild focal inflammation, no necrosis), 2: moderate (moderate density inflammation involving

195   ~10−25% area of tissue, moderate signs of early necrosis) and 3: severe (>25% area of tissue,

196   recruitment of immune cells, advanced necrotic region(s) and multiple areas of pyknosis,

197   karyolysis, and/or karyorrhexis).

198   Total RNA extraction from gill arches and anterior kidneys proceeded following Zwollo

199   et al., 2021. Briefly, RNA was purified using RNAzol RT (Sigma-Aldrich) reagent, which does

200   not require DNAse I treatment. Extracted RNA was quantified using a Nanodrop

201   spectrophotometer. RNA purity for all samples was ≥ 2.0 for 260/280, and as a secondary

202   measure, 230/280 ratios were ≥ 2.0.

203   cDNA was synthesized with iScript™ Reverse Transcriptase Supermix (Bio-Rad

204   Laboratories), using 1 ug of total RNA in a 20 uL reaction, according to manufacturer's

205   instructions. Quantitative real time polymerase chain reaction (qPCR) was used to quantify

206   number of copies of IHNV N-gene in parallel with analytical standards (Purcell et al., 2013), as

207   well as immune markers membrane-bound immunoglobulin mu (memHCmu), secreted

208 immunoglobulin mu (secHCmu), secreted immunoglobulin tau (secHCtau), interferon gamma

209 (IFNγ) and macrophage colony-stimulating factor receptor (MCSFR). Reactions were run at 25

210 µL total volume containing 1 µL of cDNA, and using 60˚C annealing temperature. Primers and

211 probe sequences and references can be found in Table S3. In general, five fish were included per

212 treatment; in certain cases, a sample was removed due to poor RNA quality, detailed in Table S2.

213 All TaqMan probe sequences (N-gene, secHCtau) were run in a single replicate per fish, while

214 SybrGreen probe sequences were ran in triplicate per fish. IHNV N-gene was expressed as the

215 log-adjusted viral RNA copy number per µg extracted RNA (Jones et al., 2020). For all immune

216 markers, the relative fold change (RFC) was calculated using critical threshold (Ct) values,

217 normalized to the no particle IHNV- control on day 31, according to Livak and Schmittgen, 2001

218 $2^{-\Delta Ct}$ method (Livak and Schmittgen, 2001), which does not require a reference gene. ARP gene

219 expression was also quantified and explored as a reference gene control, but found to be

220 differentially expressed through time, despite similar total RNA extraction yields. Differences in

221 yield were accounted for by loading the same amount of RNA in RT reactions as discussed

222 above. Tissues collected on day 56 (28 days post-IHNV exposure) were not analyzed for viral

223 load or immune gene expression.

224 *2.3 Statistical Analyses*

225 All graphical and statistical analyses were completed in R and significance was inferred

226 with $\alpha = 0.05$. For all data sets, every possible combination of fixed and random effects was

227 modeled, and the best fit model determined using Akaike Information Criterion (AIC) and

228 parsimony, with significance at $\Delta AIC \geq 2$ (R package 'stats' version 4.0.5) (RStudio Team,

229 2021). Statistical results are shown as test statistic value with factor and residual degrees of

230 freedom given as subscripts.

231   Mortality analyses were visualized with Kaplan-Meier survival curves using package

232   'survival' (Fig.1) and differences between treatments determined with Cox proportional hazard

233   models in R with the "coxph" function (RStudio Team, 2021; Therneau, 2015). The maximum

234   model tested included fixed factors of virus presence/absence (2 levels: virus, mock; categorical),

235   a 'treatment' factor in which microparticle dose and type were combined (10 levels: no particle,

236   low nylon, medium nylon, high nylon, low polystyrene, medium polystyrene, high polystyrene,

237   low spartina, medium spartina, and high spartina; categorical) and their interactions, and random

238   factor of tank. A first analysis was conducted to investigate the effect of virus exposure on

239   survival, with only the factor virus and the other factors pooled. Because no mortality was

240   observed in IHNV- treatments, a second analysis was conducted among IHNV+ fish only, to

241   avoid issues related to non-proportional hazards (same fixed and random factors) and failed

242   convergence of interactions between treatment/virus. This model was used to report significant

243   differences between IHNV+ control (no particle) and all IHNV+ particle co-exposure treatments.

244   IHNV load in water was illustrated for all tanks treated with virus for high concentration

245   only (Fig. 3A) and all concentrations in the supplement (Fig. S3). Tanks not treated with virus

246   and day 28 (day 0 after virus exposure) were not included in statistical analyses, because

247   virtually no fish had started shedding virus by day 28 and our goal was to determine how viral

248   load differed after the point shedding began. Statistical analyses were conducted with a linear

249   fixed effects model (R package 'nlme' version 3.1-152) (Pinheiro et al., 2021). The maximum

250   model tested included fixed factors as above including treatment, day (continuous variable) and

251   their interactions, and the random factor of tank; with log10(Viral RNA copies/ug RNA) as a

252   response variable. The best fitting model included treatment, day, and their interaction, as well as

253   the random influence of tank.

254   IHN viral load (log10 transformed) in gill and anterior kidney samples were analyzed

255   separately for each tissue type using a linear model (R package 'stats' version 4.0.5) (RStudio

256   Team, 2021). The maximum model included categorical factors of microparticle, collection day,

257   and their interactions. The best model for both anterior kidney and gill included the microparticle

258   treatment and collection day; the model for anterior kidney included their interaction, while gill

259   did not.

260   Gills pathological severity scale was illustrated including all fish sampled (n = 5), apart

261   from four gills that were not successfully embedded for analysis (n = 4 for spartina IHNV- day

262   31, nylon IHNV- day 42, polystyrene IHNV+ day 56, no particle IHNV+ day 56 n = 4). The

263   maximum linear model (R package 'stats' version 4.0.5) (RStudio Team, 2021) was tested

264   including all categorical factors (microparticle, virus, and day) and their interactions. The best

265   model was this maximum model, for which a three-way ANOVA was run (R package 'stats'

266   version 4.0.5) (RStudio Team, 2021). Significant differences in three-way interactions between

267   treatments were analyzed with the post-hoc Tukey honest significant differences test (R package

268   'stats' version 4.0.5) (RStudio Team, 2021), with full comparisons provided in supplementary

269   material and comparisons deemed biologically significant reported.

270   Genetic markers for immune response were evaluated using linear models (Table S2),

271   and the results of IFNγ and secreted IgT in the gill tissue graphed and analyzed separately. The

272   maximum linear model (R package 'stats' version 4.0.5) included all categorical factors of

273   microparticle, virus, day and their interactions; with ΔCt expression as a response variable. The

274   best linear model was fit to the data and included all factors but not any of their interactions.

275   Although we looked at interactions and did not find them to improve the model, power to resolve

276 them may have been limited; however, main effects are discussed and their relation to other

277 patterns observed.

278   Prior to all the analyses, data were analyzed graphically (interquartile and variance plots)

279 to validate normality and homogeneity of variance model assumptions. No outliers were found

280 that justified removal of any data points from the data set. Complete output of statistical analyses

281 and best fit models can be found in the supplementary materials. Results are typically presented

282 with subscripts on test statistic denoting factor, residual degrees of freedom. P-values were

283 rounded to the third decimal place and values less than 0.001 shown as <0.001.

284 **3. Results**

285 *3.1 Viral-mediated fish mortality*

286   Fish mortality was monitored daily (Fig. 2). There was no significant mortality (3 of 1560

287 fish dead) prior to IHNV exposure, regardless of microparticle exposure. The hazard of death

288 increased significantly (354-fold) among fish exposed to virus compared to those unexposed

289 (Cox proportional hazard analysis, $X^2_{1,17.16} = 33.73$, p-value <0.001; Fig. 2). Because virtually no

290 mortality was observed in virus negative treatments, we focused additional analyses on the virus-

291 exposed groups. Among virus-exposed fish, all microparticle types increased mortality compared

292 to no particle exposure treatments; however, the significance and magnitude of this effect

293 depended on particle type and dosage. The greatest increase in mortality was observed in the

294 high dose nylon fiber treatment (10 mg L^{-1}), reaching approximately 80%, compared to 20% for

295 fish with no microparticle exposure, increasing hazard of death by 6.4 times (Fig. 2A; $X^2_{1,15.71} =$

296 11.10, p-value < 0.001). Despite suggestive trends (i.e., p-value 0.05-0.1), the medium and low

297 nylon fiber dosages (1.0 and 0.1mg L^{-1}) did not significantly increase the hazard of death (p-

298 values >0.05). Exposure to 1 mg L^{-1} polystyrene microplastics increased the hazard of death by

15

299   3.2 times ($X^2_{1,15.71}$ = 4.10, p-value = 0.043). However, the high and low (10 or 0.1 mg L^{-1})

300   polystyrene treatments did not have a significant effect. Mortality was not significantly enhanced

301   by co-exposure to spartina microparticles at any concentration (Fig. 2C). The observed temporal

302   kinetics of mortalities was consistent between treatments and with previous *in vivo* IHNV work

303   (Wargo et al., 2010).
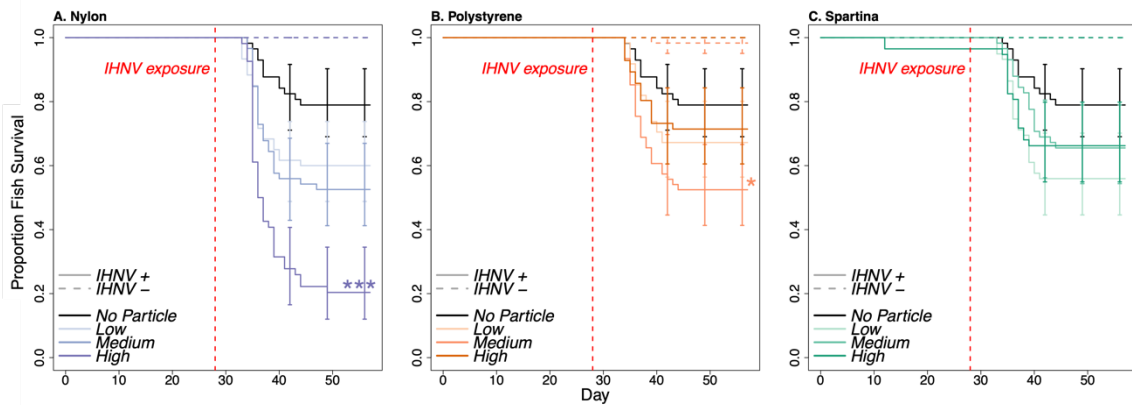
304

305   **Fig. 2. Co-exposure to IHN virus and microparticles, especially nylon fibers, resulted in**

306   **increased fish mortalities.** Most mortalities occurred between 7 and 17 days following IHNV

307   exposure, illustrated as the proportion of fish surviving over time. Virus unexposed (IHNV-,

308   dashed lines) treatments elicited little to no fish mortality, compared to virus exposed (IHNV+,

309   solid lines). Fish not exposed to any microparticles are denoted with a black line, while

310   microparticle exposures are denoted in blue (nylon, A), orange (polystyrene, B) and green

311   (spartina, C). Color shade corresponds to low (0.1 mg L^{-1}), medium (1.0 mg L^{-1}) and high (10.0

312   mg L^{-1}) microparticle exposure concentrations. Significant differences in survival between

313   IHNV+ no particle and particle treatments are denoted (Cox proportional hazard analysis, p-

314   value ≤ 0.05 : *, ≤ 0.01 : **, ≤ 0.001 : ***).

315

316   *3.2 IHNV Shedding and Body Burden*

317   Host entry, replication, and shedding are important factors in understanding viral

318   virulence, fitness, and population level spread (i.e., transmission) (Wargo and Kurath, 2012).

319   Viral shedding in surrounding tank water was quantified at ten different time points following

320   infection (Fig. 3A; all treatment data provided in Fig. S3), providing the total amount of virus

321   shed by all fish in each tank over the previous 24 hours. Previous studies have shown fish to fish

322   variation in shedding can be high, yet the kinetics of viral shed observed here are consistent with

323   traditional single-fish systems (Jones et al., 2020; Wargo et al., 2021), and treatment-level

324   differences were observed. IHNV shedding peaked two to three days post-infection and

325   significantly decreased over time (day effect, linear mixed effects model, $T_{1,229}$ = -4.9, p-value <

326   0.001) as fish died (and were removed) or survived and cleared infection. The high nylon dose

327   co-exposed fish shed significantly more virus than fish exposed to virus alone (treatment effect,

328     $T_{1,20}$ = 2.175, p-value = 0.042), unlike other microparticle co-exposures. This trend appeared to

329   be primarily driven by the peak period of viral shedding (days 1-4 post exposure to virus) (Figs.

330   2A, S3, S4).

331

17
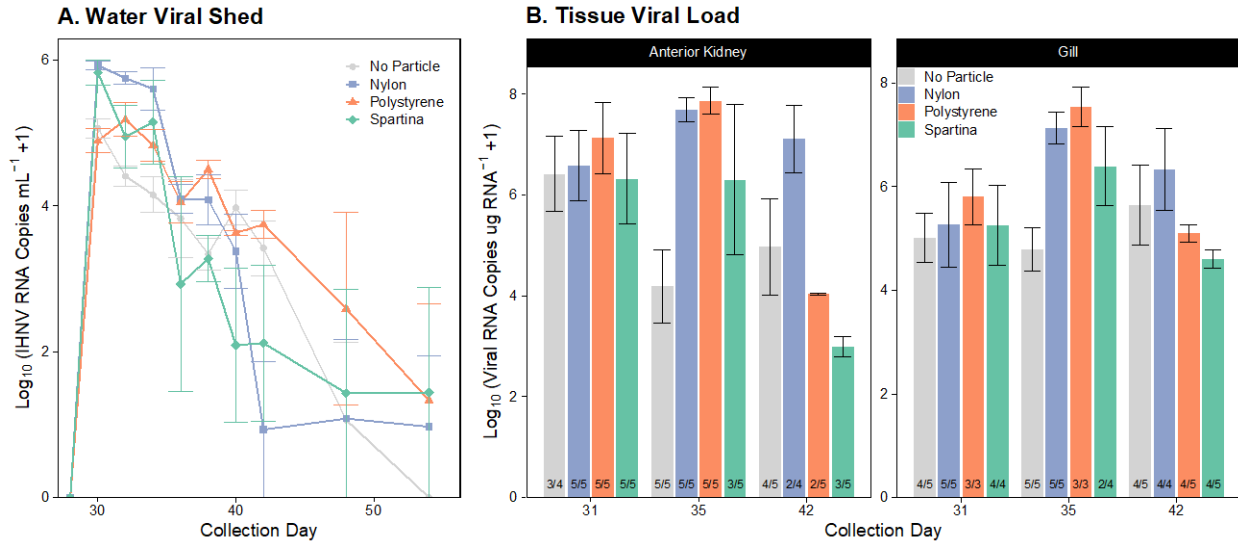
Fig. 3. Viral load in water and tissue samples over time. (A) Virus shed in water is illustrated for the high concentration of each microparticle treatment and no particle control. Points represent mean viral RNA copies uL^{-1} water of triplicate tanks per treatment ($\pm$1 standard error of mean (SEM)). Viral shed was significantly influenced by collection day (linear mixed effects model, $T_{1,229}$ = -4.9, p-value < 0.001) and higher overall in nylon co-exposed fish than those exposed to virus alone ($T_{1,20}$ = 2.175, p-value = 0.042). **(B)** IHNV loads in anterior kidney and gill tissues are presented for each collection day. Bars show mean viral RNA copies in one µg of RNA ($\pm$1 SEM) for fish terminally sampled on each day. Only fish with virus detected are included in means; number of virus positive out of total sampled are shown as ratios at the base of each bar.

Host viral tissue burden was quantified in both the anterior kidney and gill at 31, 35 and 42 days (3, 7 and 14 days post-IHNV exposure, respectively; Fig. 3B). The anterior kidney is a key site of IHNV replication and commonly analyzed to quantify IHNV body burden, while the gill is believed to be a primary point of host-entry (Drolet et al., 1994). In the anterior kidney, viral load was significantly influenced by the interaction between microparticle type and

18

349   collection day ($F_{6,35} = 2.739$, p-value = 0.027). In gills, viral load was significantly influenced by

350   nylon microfibers (linear mixed effects model, $T_{1,41} = 2.395$, p-value = 0.021). Shortly following

351   virus exposure (day 31), viral loads in the anterior kidney and gill of infected fish were similar

352   between microparticle and non-particle treatments. In the anterior kidney, tissue burden was

353   significantly higher in nylon and polystyrene co-exposed fish on day 35, compared to non-

354   particle control (Fig 2, Tukey post-hoc test, p-values = 0.029 and 0.018, respectively). This

355   appears to be driven by an increase in viral load after day 31 for fish exposed to nylon and

356   polystyrene, as well a decrease in viral load for fish not exposed to microparticles, although

357   neither of these trends were significant on their own. No other biologically significant

358   differences were observed between particle types or days in anterior kidney. In the gills, nylon

359   microfiber co-exposure had significantly higher viral loads compared to the no particle IHNV+

360   treatment, regardless of day ($T_{1,41} = 2.395$, p-value = 0.021). There was also more virus present

361   in gills on day 35 compared to day 28 across all microparticle types (day main effect, $T_{1,41} =$

362   2.284, P=0.028), in this case primarily driven by an increase in particle treatments, with little

363   decrease in no particle treatment, compared to day 31. These trends are similar when fish whose

364   tissue viral loads were below quantitation (i.e., low or no infection) were included (Fig. S5).
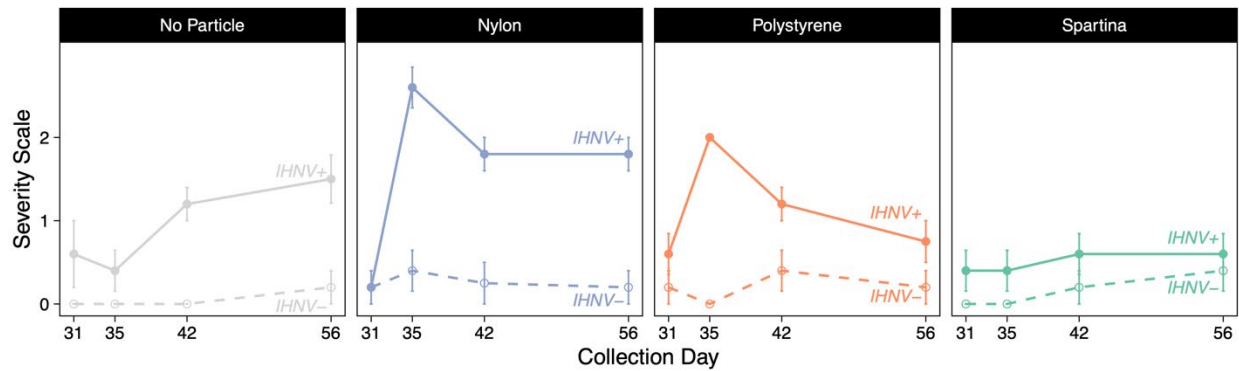
365   *3.3 Histopathology*

366   Histopathological analysis was focused on gill tissues as they are an important site of

367   IHNV entry into fish (Drolet et al., 1994). We hypothesized that increased gill pathology

368   associated with microplastic exposure may be a driver of increased mortality in fish. Gill tissues

369   were examined from the same fish for which viral loads were quantified, as well as five

370   terminally sampled fish. Each fish gill was rated on a severity scale from 0 to 3, where 3 was the

371   highest degree of observed tissue response (e.g., respiratory epithelial tissue damage,

372   inflammation, leukocyte invasion; Fig. 4A). In general, gills of fish exposed to IHNV exhibited

373   severe pathology compared to the predominantly normal healthy gill architecture (no particle

374   IHNV-; Fig 3B), significantly so for IHNV+ nylon on days 35, 42 and 56 (post-hoc Tukey's

375   honestly significant difference test p-values <0.001), IHNV+ polystyrene on day 35 (p-value <

376   0.001), and IHNV+ no particle on days 42 and 56 (p-values = 0.024 and 0.017, respectively),

377   within a given day. Spartina/virus co-exposed fish had significantly lower pathology than

378   nylon/virus co-exposed fish on days 35, 42 and 56 (p-values <0.001, 0.024 and 0.024,

379   respectively). In nylon/virus co-exposed fish, pathological severity of IHNV infection was

380   significantly higher in gills sampled on days 35, 42 and 56 than day 31 (p-values <0.001), a sign

381   of worsening infection with time. Likewise, severity of pathology increased significantly from

382   day 31 to 35 for polystyrene co-exposed fish (p-value = 0.002). This rapid increase in severity of

383   tissue pathology compared to the no particle control suggests that microplastic-exposed fish may

384   already have been in a pro-inflammatory state by the time virus challenge was initiated (day 28),

385   or this may be a function of the rapid increase in viral load at this time. It is also possible that the

386   observed increase in pathology over time may have diminished due to rapid mortality of the most

387   susceptible and diseased animals. The suggested plateau or even decrease in pathology on day 56

388   could be evidence of this phenomenon (Fig. 4). Despite such a potential bias, observed

389   pathology was still significantly higher for the nylon/virus treatment, where mortality was the

390   greatest, compared to no particle and spartina particle controls.
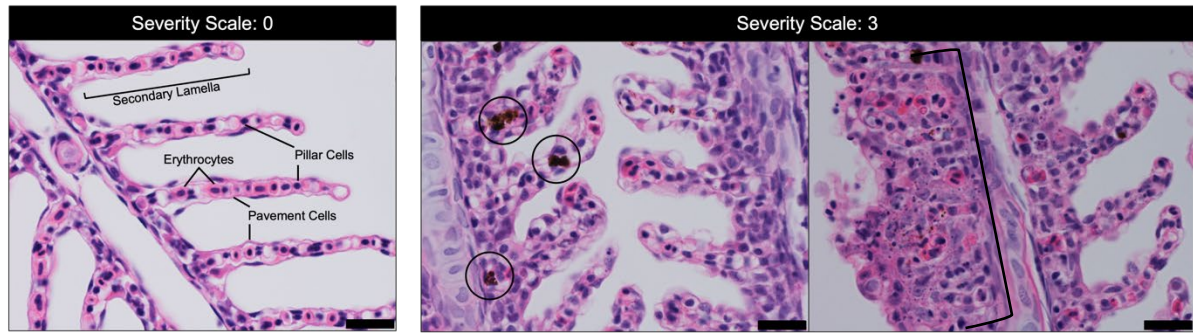
Fig. 4. Histopathological analyses of trout gill tissues. (A) Microscopic images of gill tissues

at 40 times magnification (black bar: 20 μm; Olympus AX-70 photomicroscope). Healthy tissue

(severity: 0) are on the left and unhealthy tissue sections on the right (severity: 3). Healthy tissue

exhibited normal primary gill filament and secondary lamellae cell structure. In contrast, fish

with increased pathology exhibited significant damage to the gill tissue, including widespread

respiratory epithelial cell hyperpigmentation (prominent areas circled), necrosis (bracketed

region in right severity scale 3 image), and inflammation indicated by hypertrophy, hyperplasia

and leukocytic infiltrates. **(B)** Pathological severity scale for each particle and virus treatments

(IHNV+: solid lines; IHNV-: dashed lines), averaged for each treatment with +/- 1 SEM (n = 5).

According to a three-way ANOVA, the severity of histological response was significantly

affected by the interaction between microparticle, virus, and collection day ($F_{9,124}$ = 7.631, p-

value < 0.001).

404

405   Evaluation of gill tissues in fish not exposed to IHNV was also essential, as respiration of

406   microplastic-laden water may lead to gill inflammation and pathology. Increased pathology was

407   only observed in a small subset of samples for microparticle-only exposed fish. These exhibited

408   minor sites of focal inflammation, leukocytes infiltration and epithelial damage, recorded as a

409   severity scale of 1 (Fig. 4B; Fig. S6) (Hu et al., 2020). Viral replication may have been enhanced

410   by the low-severity inflammatory response observed in fish exposed to microplastics alone and

411   supports analysis of a pro-inflammatory host response in the gills following microplastic

412   exposure. Moreover, we were unable to identify microplastic particles in histologic tissue

413   sections. This could be due to the multiple rinse steps required for excised gill arch preparation

414   or a lack of substantial microparticle integration into the tissue matrix.

415   *3.4 Immune Response*

416   To further explore gill inflammation and immune response as a cause of increased

417   disease mortality, immune gene expression was evaluated. Several genes spanning the innate and

418   adaptive branches of the immune system were measured in gill and anterior kidney of fish

419   collected for viral load analysis. The relative fold change (RFC) in expression of these genes

420   compared to the day 31 negative control (no particle, IHNV-) was analyzed following standard

421   practices (Livak and Schmittgen, 2001), illustrated for interferon gamma (IFNγ) and secreted

422   immunoglobulin tau (IgT) in gill tissues (Fig. 5). (Other markers' information is provided in

423   supplemental materials and Table S2.)

424

A. IFN γ
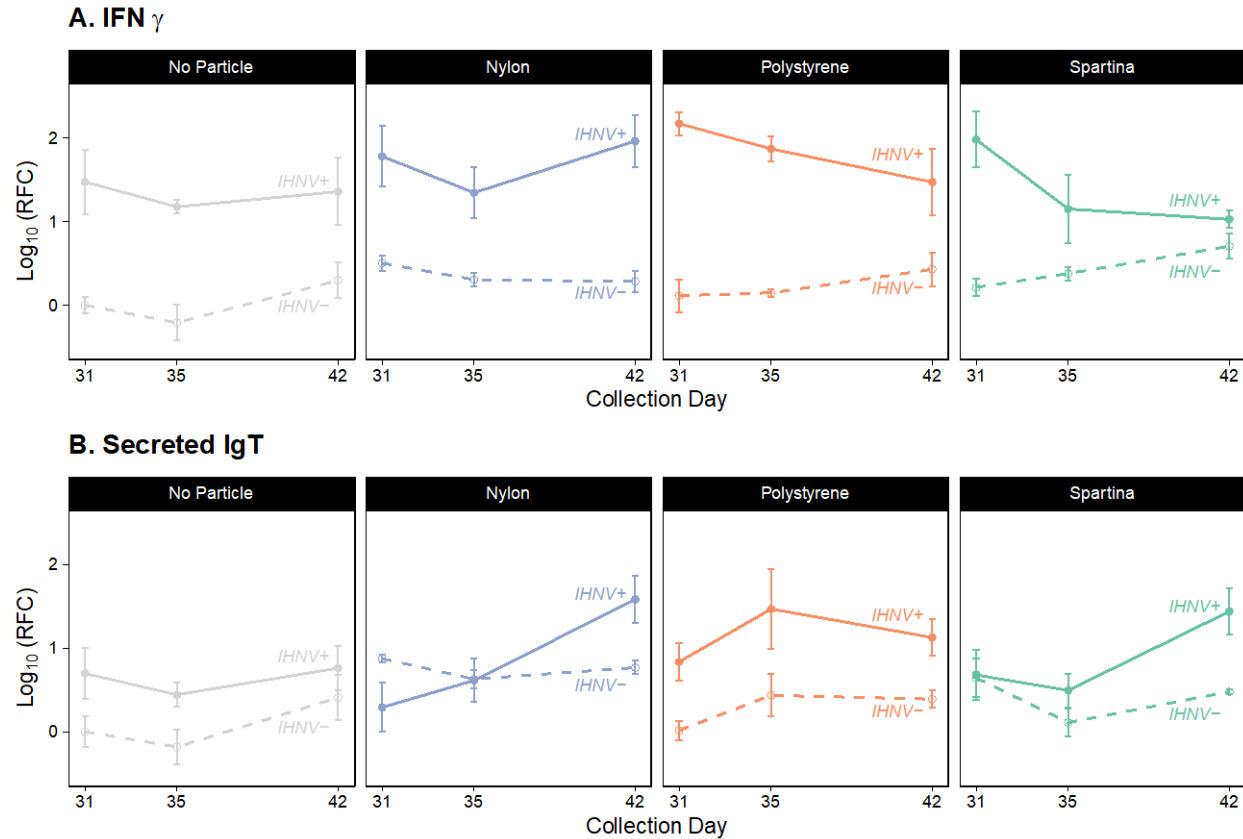
B. Secreted IgT

Fig. 5. Response of IFNγ (A) and secreted IgT (B) in gill tissue over time. The relative fold change (RFC; log10-adjusted) compared to the control (no particle, IHNV-) on day 31 is plotted for each microparticle and virus treatment on each collection day, with +/- 1 SEM (n = 5, with exceptions: Table S2). For IFNγ, expression was significantly affected by microparticle, day and virus, but not their interactions (linear mixed effects model, $F_{6,97}$ = 26.26, p-value <0.001). For secreted IgT, expression was also significantly affected by microparticle, day and virus, but not their interactions (linear mixed effects model, $F_{6,97}$ = 7.655, p-value <0.001).

IFNγ is integral in early anti-viral activity and commonly analyzed as a marker of IHNV immune response (Purcell et al., 2012, 2010). IFNγ generally triggers pro-inflammatory responses through activation of monocytes and neutrophils (Zou and Secombes, 2016). Previous

23

437   work has primarily evaluated IFNγ in hematopoietic tissues or whole-body homogenates of

438   juvenile fish, even though gills may be an important site of IHNV entry into host organisms

439   (Dixon et al., 2016; Purcell et al., 2012). We found a marked increase in IFNγ in gills of fish

440   after exposure to virus ($T_{1,97}$=11.92, p-value <0.001), in agreement with previous studies (Purcell

441   et al., 2010). Expression of IFNγ was also significantly higher in fish exposed to nylon

442   microfibers ($T_{1,97}$ = 2.42, p-value = 0.018) and polystyrene microplastics ($T_{1,97}$ = 2.20, p-value =

443   0.03), regardless of virus exposure (Fig. S7). Increased IFNγ expression suggests that

444   microplastics increased the pro-inflammatory state of gills prior to virus exposure. It is likely,

445   therefore, that microplastics acted as a mild physical irritant on the gill respiratory epithelium. To

446   further evaluate innate host defenses beyond IFNγ, we measured expression of macrophage

447   colony stimulating factor receptor (MCSFR) expression, which identifies phagocytic

448   macrophages/monocytes in teleost fishes (Takizawa et al., 2016). No differences in MCSFR

449   expression between treatment groups were observed (Table S2).

450   Secreted IgT is a key component of teleost fish mucosal antibody response (Purcell et al.,

451   2012). Our results demonstrate that infection with IHNV significantly increased secreted IgT

452   expression compared to uninfected fish ($T_{1,97}$ = 4.56, p-value < 0.001), indicating that there was a

453   mucosal antibody response to IHNV in the gills. This response increased over time, as

454   demonstrated by significantly increased expression from day 31 to 42 ($T_{1,\,97}$ = 3.01, p-value =

455   0.003). This pattern of initially low and increased expression through time appeared to be most

456   pronounced in the nylon microfiber and IHNV co-exposed fish (and to a lesser degree, spartina

457   microparticle co-exposed fish), suggesting potential delay in secreted IgT response, although

458   there was no statistical interaction between time, microparticle, and/or virus exposure. Secreted

459   IgT expression was significantly higher among fish exposed to nylon, polystyrene or spartina

460   microparticles ($T_{1,97}$ = 2.81, 2.36, 2.08, and p-values = 0.006, 0.02 and 0.04, respectively) than

461   those not exposed to microparticles, regardless of IHNV exposure (Fig. S8). This suggests that

462   the presence of microparticles increased the mucosal antibody response but that this activation

463   was not protective, as co-exposure to virus and microplastics is correlated with both increased

464   viral load/shedding and mortality in our study. This agrees with other research that has shown

465   correlations between level of inflammation, pathogen load, and disease expression (Quddos and

466   Zwollo, 2021). In addition to secreted IgT, secreted and membrane-bound forms of the more

467   systemic immunoglobulin Mu (IgM) were also analyzed to assess humoral immune response,

468   because *in vitro* work suggested that B-lymphoid development in the anterior kidney was

469   suppressed by the presence of the polystyrene microplastics (Yang, 2020; Zwollo et al., 2021)..

470   We did not observe any change in expression of the membrane form of immunoglobulin mu

471   between treatments in anterior kidney tissues (Table S2). The response was highly variable

472   between sampling times, suggesting our analyses may not have had sufficient temporal

473   resolution or power (limited sample size) to distinguish any relationship between humoral

474   immunity and microparticle exposure *in vivo*. Effects to B-lymphopoeisis sould be most

475   pronounced if microparticles translocated to the tissue of the anterior kidney, but this was not

476   examined in this study.

477

478   **4. DISCUSSION**

479   Assessment of the risks of microplastic exposure must consider that, in the actual

480   environment, organisms are subject to multiple stressors (e.g., pathogens, toxic chemicals,

481   altered temperature and pH), not just microplastics alone. We hypothesized that microplastics

482   would increase IHNV virulence, while the natural microparticle (spartina) would have no effect

483   – a product of particle chemistry (natural polymer v. synthetic polymers with chemical

484   additives). Our results were consistent with this hypothesis as only microplastics (nylon

485   microfibers and polystyrene microplastics) had a significant effect on virulence. Toxicity may

486   derive from chemical constituents (Zimmermann et al., 2019), or more simply the higher

487   crystallinity (i.e., hardness) common in synthetic polymers (Andrady, 2017). Expanded

488   polystyrene is commonly used in buoys and floats, as well as single use containers and shipping

489   packaging (Darnerud, 2003; Jang et al., 2017). The polystyrene used here was produced for

490   home insulation and contained the brominated flame retardant hexabromocyclododecane. The

491   nylon microfibers were free of known additives, apart from TiO_2 as a delustrant (manufacturer

492   reported). Spartina is a lignocellulose-based polymer (Hodson et al., 1984). The microparticle

493   treatments with the greatest influence on IHNV virulence (polystyrene and nylon) were

494   composed of petroleum-based polymers, but the expected toxicity of their additives (i.e.,

495   hexabromocyclododecane) did not correlate with mortality. This suggests that the physical

496   properties of the microplastics drove effects more than the chemical additive constituents. We

497   note that our experimental design (i.e., tank flushing and dosing every other day) may have

498   diminished possible leachate effect compared to environments where polluted plastic

499   concentrations are chronically high, which is difficult to simulate in a laboratory setting *in vivo*.

500   However, microplastic and leachate concentrations in the environment can be highly variable

501   through time, due to tidal, circulation, or variable inputs (Hale et al., 2020). How this variability

502   influences disease dynamics would be an exciting are of research.

503   The size and shape of nylon microfibers may also be important drivers of IHNV-induced

504   mortality. Indeed, recent work propounds that microfibers have distinct toxicological impacts

505   (Bucci and Rochman, 2022). Although it is often speculated that smaller particles may have the

506   greatest magnitude of effect due to cellular-level interactions, the polystyrene and spartina in our

507   study were similarly small but enhanced mortality less so than nylon microfibers (Besseling et

508   al., 2019). We calculated (using particle sizes and densities) that our mass-based exposures

509   equated to nearly 100-fold fewer nylon microfibers (approximately 29,000 to 290) than

510   polystyrene microplastics (2,400,000 to 24,000) per liter. This underscores the relative potency

511   of the nylon microfibers; that is, fewer microfibers caused a greater effect than more numerous

512   polystyrene microplastics. By using a large range of doses, we spanned possible environmental

513   concentrations, which are typically stochastic and are likely underestimated due to sampling and

514   analytical biases (Hale et al., 2020).

515   Interestingly, virulence response to nylon microfiber exposure followed a clear dose

516   response, while polystyrene did not. Although dose generally correlates with toxicity, the

517   absence of a dose response in polystyrene-exposed fish may indicate that smaller microparticles

518   (polystyrene and spartina) might have aggregated in water at high doses, effectively decreasing

519   the number of 'particles' to which an organism is exposed. Microplastic agglomeration can be

520   influenced by size, surface charge/chemistry, biofilm formation, microplastic concentration and

521   salinity (Shupe et al., 2021; Summers et al., 2018). We cannot exclude this hypothesis as no

522   mechanisms beyond aeration were used to disperse particles, even though particles were visually

523   observed to disperse within tanks. We do not believe that the lack of a dose response was a result

524   of variation between tanks or individual fish within tanks because this was accounted for in our

525   models by including tank as a random effect (model 1: $X^2_{13.93,17.16} = 34.33$, p-value = 0.002;

526   model 2: $X^2_{13.52,15.71} = 33.82$, p-value = 0.002).

527   The data presented on viral shedding and host viral load support the conclusion that host

528   viral replication increased and, perhaps more importantly, clearance rate decreased when fish

529   were co-exposed to virus and microplastics (especially nylon microfibers and polystyrene

530   microplastics), leading to exacerbated disease and mortality. This resulted in more viral shedding

531   in the nylon co-exposure. Together, this suggests that the increased mortality associated with

532   exposure to microplastics was driven by higher viral loads for a longer period of time, as well as

533   possibly compromised tolerance for the same viral load. Again, co-exposed microparticle type

534   was an important driver of these dynamics, with nylon having the most pronounced effect. These

535   data agree with previous work that IHNV *in vivo* fitness, particularly duration of infection, can

536   correlate with virulence in fish (Jones et al., 2020; Wargo et al., 2021, 2017, 2010). Further, the

537   increase in shedding following nylon and viral co-exposure suggests that between-host

538   transmission may also be increased by microplastic co-exposure. This has major epidemiological

539   implications for the spread and burden of disease at a population level.

540   Enhanced in-host and shed viral load among microplastic and virus co-exposed fish was

541   associated with tissue damage . Expression of select markers indicative of host defense

542   mechanisms suggest that microplastic/IHNV co-exposed fish did not exhibit plastic-induced

543   immunosuppression of the marker genes analyzed here. Rather, there was evidence of a pro-

544   inflammatory immune response among uninfected fish exposed to microparticles, particularly

545   microfibers. In addition, although phagocytic cells (including macrophages, monocytes,

546   granulocytic cells, and phagocytic B cells) have been documented to engulf microplastics ≤10

547   µm *in vitro* (Zwollo et al., 2021), the number of polystyrene or spartina particles of this size

548   encountering fish gills may have been insufficient to trigger a phagocytic response detectable by

549   MCSFR. Neutrophil marker myeloperoxidase (MPO) should be investigated in future work.

550   One explanation for these results is that microparticles lead to enhanced host viral entry

551   (initially into host barrier epithelial cells) and stress, which lead to reduced viral clearance, when

552   microparticles were present (Fig. 6). Successful host colonization is the first step in establishing

553   infection, to which fish present both physical and immunological defenses (Salinas, 2015; Wargo

554   and Kurath, 2011). Here, microparticles may have damaged epithelia after contact with

555   respiratory surfaces or the digestive tract, if ingested (as demonstrated by Hu et al., 2020) – both

556   sites of IHNV possible host invasion (Bour et al., 2020; Dixon et al., 2016; Hu et al., 2020).

557   Similarly, such tissue damage may cause a proinflammatory or other response in host, and allow

558   for greater IHNV replication or reduced efficacy in virus clearance. The likelihood that a particle

559   could damage associated epithelia and cause stress may be a function of its physical properties.

560   Synthetic polymers may be less flexible (more crystalline) than natural materials (Andrady,

561   2017). Shape may also be critical; asbestos and workers lung are a product of the particle shape,

562   not chemistry (Pimentel et al., 1975; Siegrist and Wylie, 1980). Recent research has found that

563   microplastics can cause intestinal abrasion, and that longer plastic microfibers (≤ 200 μm) may be

564   more damaging (Zhao et al., 2021). This may explain why smaller polystyrene microplastics

565   enhanced virulence of IHNV (and without a clear dose response), but less so than nylon

566   microfibers, and warrants further investigation. Duration of microparticle exposure prior to

567   pathogen should also be considered; longer exposure times may result in increased tissue damage

568   and inflammation, as seen here, versus shorter exposures without microplastic exposure prior to

569   pathogen introduction (Leads et al., 2019). Further, although microplastic biofilms have been

570   proposed as a viral vector which could enhance exposure pathways (Amaral-Zettler et al., 2020),

571   our fish were actually exposed to IHNV in the absence of microparticles (plastic dosing occurred

572   before and after viral exposure). In a separate *in vitro* study, we observed that viral load was not

573   affected by the presence of microparticles over 48 hours. This indicates that microparticle

574   sorption, leached additives, or unbound monomers did not influence viral exposure

575 concentrations (Fig. S9). Based on the data gathered here, enhanced host colonization or viral

576 replication caused by physical interactions of the host with microparticles (particularly

577 microfibers) seems a probable explanation, but warrants further investigation.

578

Virus Only   Virus + Microparticle   Virus + Microfiber
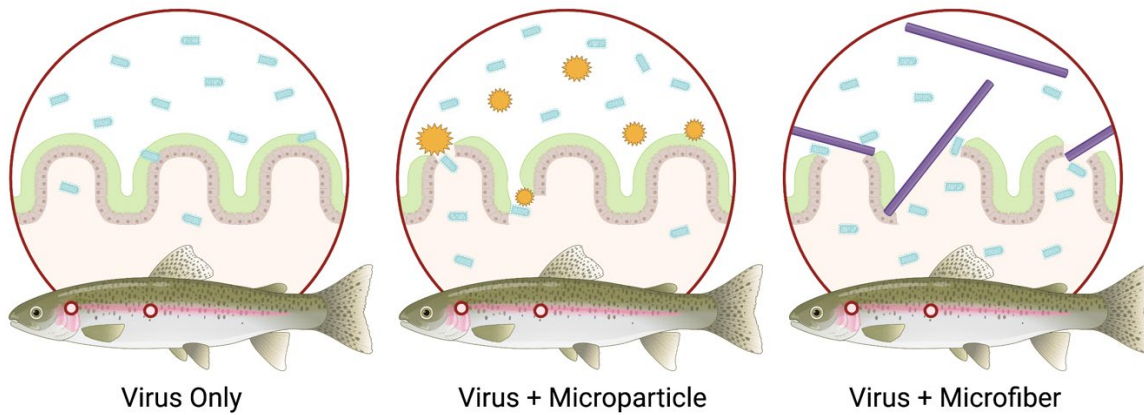
580 **Fig. 6. Proposed mechanism of microplastics increased virulence.** When exposed to virus

581 alone (blue virions), mucosal and epithelial barriers of the gill and intestinal tract block some

582 virus from entering the tissues. When exposed to microparticles and then virus, the

583 epithelial/mucosal barrier may incur mild physical damage to membranes causing inflammatory

584 response. Damage is greater for microfibers, which are larger and may be more likely to become

585 entrapped in and damage the outer membrane of delicate epithelia. This may facilitate greater

586 viral entry and host stress (facilitating greater viral replication and reductions in clearance),

587 ultimately increasing disease virulence. Illustration not to scale.

588

589 **5. Conclusions**

590   Overall, our results demonstrate that exposure to microplastics increased lethality of a

591 serious infectious disease in an economically important fish species. This effect was most

592 pronounced for nylon microfibers. To explore this finding, we evaluated viral shedding, host

593 viral load, histopathology of the gills and aspects of immune response. We found that fish co-

594 exposed to the highest concentration of nylon microfibers and virus had a greater viral load and

595 shedding, more tissue damage on gills, and pro-inflammatory immune response. Therefore, we

596 hypothesize that the increase lethality of virus in this co-exposure was caused by greater

597 infection severity. Our results have substantial implications, given the widespread distribution

598 and increasing concentrations of microplastics, particularly microfibers. The proposed

599 interactions between microplastics, pathogens and hosts merit further investigation. Importantly,

600 the characteristics of microplastics (i.e., size, shape, chemistry, crystallinity) responsible for

601 eliciting detrimental effects should be explored. The question of whether microparticles of a

602 larger size or microfibers of a natural material cause similar damage also remains open. Our

603 results also indicated microplastic co-exposure may enhance viral transmission. This could have

604 major epidemiological consequences, such as increase pathogen prevalence and spillover from

605 plastic-exposed to non-exposed populations. Our findings have implications across a range of

606 aquatic and terrestrial host-pathogen systems. This includes humans, who are also coincidentally

607 exposed to microplastics and infectious agents in indoor environments (Prata et al., 2020); the

608 latter has been dramatically illustrated in the case of the SARS-CoV-2 virus (Chen et al., 2021).

609 Host and pathogen systems such as the one used here can serve as a model for the relationship

610 between pathogens and microplastics, and interdisciplinary work regarding the mechanisms

611 underlying this relationship should be prioritized. This study supports the supposition that

612 microplastics may be a global threat, of which the ramifications must be considered in the

613 context of multiple stressors and realistic ecosystems.

614

615 **Acknowledgements**

627   **CRediT authorship contribution statement**

628   MES contributed to conceptualization, methodology, formal analysis, investigation, data

629   curation, writing – original draft, writing – review & editing, visualization, project

630   administration, funding acquisition. RCH contributed to conceptualization, methodology,

631   resources, writing – review & editing, supervision, project administration, funding acquisition.

632   PXZ contributed to conceptualization, methodology, resources, writing – review & editing,

633   visualization, project administration, funding acquisition. WKV contributed to conceptualization,

634   methodology, resources, writing – review & editing, visualization, project administration,

635   funding acquisition. GV contributed to investigation and data curation. ARW contributed to

636   conceptualization, methodology, formal analysis, resources, writing – review & editing,

637   supervision, project administration, funding acquisition.

638

References

640   Amaral-Zettler, L.A., Zettler, E.R., Mincer, T.J., 2020. Ecology of the plastisphere. Nat. Rev.
641   Microbiol. 18, 139–151. https://doi.org/10.1038/s41579-019-0308-0

642   Andrady, A.L., 2017. The plastic in microplastics: A review. Mar. Pollut. Bull. 119, 12–22.
643   https://doi.org/10.1016/j.marpolbul.2017.01.082

644   Athey, S.N., Erdle, L.M., 2021. Are We Underestimating Anthropogenic Microfiber Pollution?
645   A Critical Review of Occurrence, Methods, and Reporting. Environ. Toxicol. Chem. 41,
646   822–837. https://doi.org/10.1002/etc.5173

647   Besseling, E., Redondo-Hasselerharm, P., Foekema, E.M., Koelmans, A.A., 2019. Quantifying
648   ecological risks of aquatic micro- and nanoplastic. Crit. Rev. Environ. Sci. Technol. 49,
649   32–80. https://doi.org/10.1080/10643389.2018.1531688

650   Bootland, L., Leong, J.-A., 2011. Infectious haematopoietic necrosis virus, in: Fish Diseases and
651   Disorders. pp. 66–109.

652   Borrelle, S.B., Ringma, J., Law, K.L., Monnahan, C.C., Lebreton, L., McGivern, A., Murphy, E.,
653   Jambeck, J., Leonard, G.H., Hilleary, M.A., Eriksen, M., Possingham, H.P., De Frond,
654   H., Gerber, L.R., Polidoro, B., Tahir, A., Bernard, M., Mallos, N., Barnes, M., Rochman,
655   C.M., 2020. Predicted growth in plastic waste exceeds efforts to mitigate plastic
656   pollution. Science 369, 1515–1518. https://doi.org/10.1126/science.aba3656

657   Bour, A., Hossain, S., Taylor, M., Sumner, M., Carney Almroth, B., 2020. Synthetic Microfiber
658   and Microbead Exposure and Retention Time in Model Aquatic Species Under Different
659   Exposure Scenarios. Front. Environ. Sci. 8, 83. https://doi.org/10.3389/fenvs.2020.00083

660   Bucci, K., Rochman, C.M., 2022. Microplastics: a multidimensional contaminant requires a
661   multidimensional framework for assessing risk. Microplastics Nanoplastics 2, 7.
662   https://doi.org/10.1186/s43591-022-00028-0

663   Bucci, K., Tulio, M., Rochman, C.M., 2020. What is known and unknown about the effects of
664   plastic pollution: A meta-analysis and systematic review. Ecol. Appl. 30, e02044.
665   https://doi.org/10.1002/eap.2044

666   Chen, B., Jia, P., Han, J., 2021. Role of indoor aerosols for COVID-19 viral transmission: a
667   review. Environ. Chem. Lett. 19, 1953–1970. https://doi.org/10.1007/s10311-020-01174-
668   8

669   Darnerud, P.O., 2003. Toxic effects of brominated flame retardants in man and in wildlife.
670   Environ. Int. 29, 841–853. https://doi.org/10.1016/S0160-4120(03)00107-7

671   Dixon, P., Paley, R., Alegria-Moran, R., Oidtmann, B., 2016. Epidemiological characteristics of
672   infectious hematopoietic necrosis virus (IHNV): a review. Vet. Res. 47, 63.
673   https://doi.org/10.1186/s13567-016-0341-1

674   Drolet, B.S., Rohovec, J.S., Leong, J.C., 1994. The route of entry and progression of infectious
675   haematopoietic necrosis virus in Oncorhynchus mykiss (Walbaum): a sequential
676   immunohistochemical study. J. Fish Dis. 17, 337–344. https://doi.org/10.1111/j.1365-
677   2761.1994.tb00229.x

678   Everson, J.L., Jones, D.R., Taylor, A.K., Rutan, B.J., Leeds, T.D., Langwig, K.E., Wargo, A.R.,
679   Wiens, G.D., 2021. Aquaculture Reuse Water, Genetic Line, and Vaccination Affect
680   Rainbow Trout (Oncorhynchus mykiss) Disease Susceptibility and Infection Dynamics.
681   Front. Immunol. 12, 3894. https://doi.org/10.3389/fimmu.2021.721048

682 Gauthier, D., Haines, A., Vogelbein, W., 2021. Elevated temperature inhibits Mycobacterium
683   shottsii infection and Mycobacterium pseudoshottsii disease in striped bass Morone
684   saxatilis. Dis. Aquat. Organ. 144, 159–174. https://doi.org/10.3354/dao03584
685 Geyer, R., Jambeck, J.R., Law, K.L., 2017. Production, use, and fate of all plastics ever made.
686   Sci. Adv. 3, e1700782. https://doi.org/10.1126/sciadv.1700782
687 Hale, R.C., Seeley, M.E., La Guardia, M.J., Mai, L., Zeng, E.Y., 2020. A Global Perspective on
688   Microplastics. J. Geophys. Res. Oceans 125, e2018JC014719.
689   https://doi.org/10.1029/2018JC014719
690 Hodson, R., Christian, R., Maccubbin, A., 1984. Lignocellulose and lignin in the salt marsh grass
691   Spartina alterniflora: initial concentrations and short-term, post-depositional changes in
692   detrital matter 81, 1–7. https://doi.org/10.1007/BF00397619
693 Hu, L., Chernick, M., Lewis, A.M., Ferguson, P.L., Hinton, D.E., 2020. Chronic microfiber
694   exposure in adult Japanese medaka (Oryzias latipes). PLOS ONE 15, e0229962.
695   https://doi.org/10.1371/journal.pone.0229962
696 Jang, M., Shim, W.J., Han, G.M., Rani, M., Song, Y.K., Hong, S.H., 2017. Widespread detection
697   of a brominated flame retardant, hexabromocyclododecane, in expanded polystyrene
698   marine debris and microplastics from South Korea and the Asia-Pacific coastal region.
699   Environ. Pollut. 231, 785–794. https://doi.org/10.1016/j.envpol.2017.08.066
700 Jennings, S., Stentiford, G.D., Leocadio, A.M., Jeffery, K.R., Metcalfe, J.D., Katsiadaki, I.,
701   Auchterlonie, N.A., Mangi, S.C., Pinnegar, J.K., Ellis, T., Peeler, E.J., Luisetti, T., Baker-
702   Austin, C., Brown, M., Catchpole, T.L., Clyne, F.J., Dye, S.R., Edmonds, N.J., Hyder,
703   K., Lee, J., Lees, D.N., Morgan, O.C., O'Brien, C.M., Oidtmann, B., Posen, P.E., Santos,
704   A.R., Taylor, N.G.H., Turner, A.D., Townhill, B.L., Verner-Jeffreys, D.W., 2016.
705   Aquatic food security: insights into challenges and solutions from an analysis of
706   interactions between fisheries, aquaculture, food safety, human health, fish and human
707   welfare, economy and environment. Fish Fish. 17, 893–938.
708   https://doi.org/10.1111/faf.12152
709 Jones, D.R., Rutan, B.J., Wargo, A.R., 2020. Impact of Vaccination and Pathogen Exposure
710   Dosage on Shedding Kinetics of Infectious Hematopoietic Necrosis Virus (IHNV) in
711   Rainbow Trout. J. Aquat. Anim. Health 32, 95–108. https://doi.org/10.1002/aah.10108
712 Lamb, J.B., Willis, B.L., Fiorenza, E.A., Couch, C.S., Howard, R., Rader, D.N., True, J.D.,
713   Kelly, L.A., Ahmad, A., Jompa, J., Harvell, C.D., 2018. Plastic waste associated with
714   disease on coral reefs. Science 359, 460–462. https://doi.org/10.1126/science.aar3320
715 Leads, R.R., Burnett, K.G., Weinstein, J.E., 2019. The Effect of Microplastic Ingestion on
716   Survival of the Grass Shrimp *Palaemonetes pugio* (Holthuis, 1949) Challenged with
717   *Vibrio campbellii*. Environ. Toxicol. Chem. 38, 2233–2242.
718   https://doi.org/10.1002/etc.4545
719 Leslie, H.A., J. M. van Velzen, M., Brandsma, S.H., Vethaak, D., Garcia-Vallejo, J.J., Lamoree,
720   M.H., 2022. Discovery and quantification of plastic particle pollution in human blood.
721   Environ. Int. 163, 107199. https://doi.org/10.1016/j.envint.2022.107199
722 Livak, K.J., Schmittgen, T.D., 2001. Analysis of Relative Gene Expression Data Using Real-
723   Time Quantitative PCR and the 2−ΔΔCT Method. Methods 25, 402–408.
724   https://doi.org/10.1006/meth.2001.1262
725 MacLeod, M., Arp, H.P.H., Tekman, M.B., Jahnke, A., 2021. The global threat from plastic
726   pollution. Science 373, 61–65. https://doi.org/10.1126/science.abg5433

727 Pimentel, J.C., Avila, R., Lourenço, A.G., 1975. Respiratory disease caused by synthetic fibres: a
728   new occupational disease. Thorax 30, 204–219.
729 Pinheiro, J., Bates, D., DebRoy, S., Sakar, D., 2021. _nlme: Linear and Nonlinear Mixed Effects
730   Models_. R package version 3.1-152.
731 Prata, J.C., da Costa, J.P., Lopes, I., Duarte, A.C., Rocha-Santos, T., 2020. Environmental
732   exposure to microplastics: An overview on possible human health effects. Sci. Total
733   Environ. 702, 134455. https://doi.org/10.1016/j.scitotenv.2019.134455
734 Purcell, M., Thompson, R., Garver, K., Hawley, L., Batts, W., Sprague, L., Sampson, C.,
735   Winton, J., 2013. Universal reverse-transcriptase real-time PCR for infectious
736   hematopoietic necrosis virus (IHNV). Dis. Aquat. Organ. 106, 103–115.
737   https://doi.org/10.3354/dao02644
738 Purcell, M.K., Laing, K.J., Winton, J.R., 2012. Immunity to Fish Rhabdoviruses. Viruses 4, 140–
739   166. https://doi.org/10.3390/v4010140
740 Purcell, M.K., LaPatra, S.E., Woodson, J.C., Kurath, G., Winton, J.R., 2010. Early viral
741   replication and induced or constitutive immunity in rainbow trout families with
742   differential resistance to Infectious hematopoietic necrosis virus (IHNV). Fish Shellfish
743   Immunol. 28, 98–105. https://doi.org/10.1016/j.fsi.2009.10.005
744 Quddos, F., Zwollo, P., 2021. A BCWD-Resistant line of rainbow trout is less sensitive to
745   cortisol implant-induced changes in IgM response as compared to a susceptible (control)
746   line. Dev. Comp. Immunol. 116, 103921. https://doi.org/10.1016/j.dci.2020.103921
747 Ragusa, A., Svelato, A., Santacroce, C., Catalano, P., Notarstefano, V., Carnevali, O., Papa, F.,
748   Rongioletti, M.C.A., Baiocco, F., Draghi, S., D'Amore, E., Rinaldo, D., Matta, M.,
749   Giorgini, E., 2021. Plasticenta: First evidence of microplastics in human placenta.
750   Environ. Int. 146, 106274. https://doi.org/10.1016/j.envint.2020.106274
751 Rochman, C.M., Brookson, C., Bikker, J., Djuric, N., Earn, A., Bucci, K., Athey, S., Huntington,
752   A., McIlwraith, H., Munno, K., De Frond, H., Kolomijeca, A., Erdle, L., Grbic, J.,
753   Bayoumi, M., Borrelle, S.B., Wu, T., Santoro, S., Werbowski, L.M., Zhu, X., Giles, R.K.,
754   Hamilton, B.M., Thaysen, C., Kaura, A., Klasios, N., Ead, L., Kim, J., Sherlock, C., Ho,
755   A., Hung, C., 2019. Rethinking microplastics as a diverse contaminant suite. Environ.
756   Toxicol. Chem. 38, 703–711. https://doi.org/10.1002/etc.4371
757 RStudio Team, 2021. _RStudio: Integrated Development Environment for R_.
758 Salinas, I., 2015. The Mucosal Immune System of Teleost Fish. Biology 4, 525–539.
759   https://doi.org/10.3390/biology4030525
760 Seeley, M.E., Song, B., Passie, R., Hale, R.C., 2020. Microplastics affect sedimentary microbial
761   communities and nitrogen cycling. Nat. Commun. 11, 2372.
762   https://doi.org/10.1038/s41467-020-16235-3
763 Shupe, H.J., Boenisch, K.M., Harper, B.J., Brander, S.M., Harper, S.L., 2021. Effect of
764   Nanoplastic Type and Surface Chemistry on Particle Agglomeration over a Salinity
765   Gradient. Environ. Toxicol. Chem. 40, 1820–1826. https://doi.org/10.1002/etc.5030
766 Siegrist, H.G., Wylie, A.G., 1980. Characterizing and discriminating the shape of asbestos
767   particles. Environ. Res. 23, 348–361.
768 Springman, K.R., Kurath, G., Anderson, J.J., Emlen, J.M., 2005. Contaminants as viral cofactors:
769   assessing indirect population effects. Aquat. Toxicol. 71, 13–23.
770   https://doi.org/10.1016/j.aquatox.2004.10.006

771   Summers, S., Henry, T., Gutierrez, T., 2018. Agglomeration of nano- and microplastic particles
772   in seawater by autochthonous and de novo-produced sources of exopolymeric substances.
773   Mar. Pollut. Bull. 130, 258–267. https://doi.org/10.1016/j.marpolbul.2018.03.039
774   Takizawa, F., Magadan, S., Parra, D., Xu, Z., Korytář, T., Boudinot, P., Sunyer, J.O., 2016.
775   Novel Teleost CD4-Bearing Cell Populations Provide Insights into the Evolutionary
776   Origins and Primordial Roles of CD4+ Lymphocytes and CD4+ Macrophages. J.
777   Immunol. 196, 4522–4535. https://doi.org/10.4049/jimmunol.1600222
778   Therneau, T., 2015. A package for survival analysis in S, version 2.38.
779   Wargo, A.R., Garver, K.A., Kurath, G., 2010. Virulence correlates with fitness in vivo for two M
780   group genotypes of Infectious hematopoietic necrosis virus (IHNV). Virology 404, 51–
781   58. https://doi.org/10.1016/j.virol.2010.04.023
782   Wargo, A.R., Kurath, G., 2012. Viral fitness: definitions, measurement, and current insights.
783   Curr. Opin. Virol. 2, 538–545. https://doi.org/10.1016/j.coviro.2012.07.007
784   Wargo, A.R., Kurath, G., 2011. In Vivo Fitness Associated with High Virulence in a Vertebrate
785   Virus Is a Complex Trait Regulated by Host Entry, Replication, and Shedding. J. Virol.
786   85, 3959–3967. https://doi.org/10.1128/JVI.01891-10
787   Wargo, A.R., Kurath, G., Scott, R.J., Kerr, B., 2021. Virus shedding kinetics and unconventional
788   virulence tradeoffs. PLOS Pathog. 17, e1009528.
789   https://doi.org/10.1371/journal.ppat.1009528
790   Wargo, A.R., Scott, R.J., Kerr, B., Kurath, G., 2017. Replication and shedding kinetics of
791   infectious hematopoietic necrosis virus in juvenile rainbow trout. Virus Res. 227, 200–
792   211. https://doi.org/10.1016/j.virusres.2016.10.011
793   Yang, H., 2020. Polystyrene microplastics decrease F-53B bioaccumulation but induce
794   inflammatory stress in larval zebrafish. Chemosphere 8.
795   https://doi.org/10.1016/j.chemosphere.2020.127040
796   Zhao, Y., Qiao, R., Zhang, S., Wang, G., 2021. Metabolomic profiling reveals the intestinal
797   toxicity of different length of microplastic fibers on zebrafish (Danio rerio). J. Hazard.
798   Mater. 403, 123663. https://doi.org/10.1016/j.jhazmat.2020.123663
799   Zimmermann, L., Dierkes, G., Ternes, T.A., Völker, C., Wagner, M., 2019. Benchmarking the in
800   Vitro Toxicity and Chemical Composition of Plastic Consumer Products. Environ. Sci.
801   Technol. 53, 11467–11477. https://doi.org/10.1021/acs.est.9b02293
802   Zou, J., Secombes, C., 2016. The Function of Fish Cytokines. Biology 5, 23.
803   https://doi.org/10.3390/biology5020023
804   Zwollo, P., Quddos, F., Bagdassarian, C., Seeley, M.E., Hale, R.C., Abderhalden, L., 2021.
805   Polystyrene microplastics reduce abundance of developing B cells in rainbow trout
806   (Oncorhynchus mykiss) primary cultures. Fish Shellfish Immunol. 114, 102–111.
807   https://doi.org/10.1016/j.fsi.2021.04.014
808